

Article

Preparation of Chiral Porous Organic Cage Clicked Chiral Stationary Phase for HPLC Enantioseparation

Ya-Nan Gong , Qi-Yu Ma, Ying Wang, Jun-Hui Zhang * , You-Ping Zhang, Rui-Xue Liang, Bang-Jin Wang *, Sheng-Ming Xie and Li-Ming Yuan

Department of Chemistry, Yunnan Normal University, Kunming 650500, China

* Correspondence: zhangjunhui@ynnu.edu.cn (J.-H.Z.); wangbangjin@ynnu.edu.cn (B.-J.W.)

Abstract: Porous organic cages (POCs) are a new subclass of porous materials, which are constructed from discrete cage molecules with permanent cavities via weak intermolecular forces. In this study, a novel chiral stationary phase (CSP) has been prepared by chemically binding a [4 + 6]-type chiral POC (C₁₂₀H₉₆N₁₂O₄) with thiol-functionalized silica gel using a thiol-ene click reaction and applied to HPLC separations. The column packed with this CSP presented good separation capability for chiral compounds and positional isomers. Thirteen racemates have been enantioseparated on this column, including alcohols, diols, ketones, amines, epoxides, and organic acids. Upon comparison with a previously reported chiral POC NC1-R-based column, commercial Chiralpak AD-H, and Chiralcel OD-H columns, this column is complementary to these three columns in terms of its enantiomeric separation; and can also separate some racemic compounds that cannot be separated by the three columns. In addition, eight positional isomers (iodoaniline, bromoaniline, chloroaniline, dibromobenzene, dichlorobenzene, toluidine, nitrobromobenzene, and nitroaniline) have also been separated. The influences of the injection weight and column temperature on separation have been explored. After the column has undergone multiple injections, the relative standard deviations (RSDs) for the retention time and selectivity were below 1.0 and 1.5%, respectively, indicating the good reproducibility and stability of the column for separation. This work demonstrates that POCs are promising materials for HPLC separation.

Keywords: chiral porous organic cage; high performance liquid chromatography; chiral stationary phase; enantioseparation; thiol-ene click reaction



Citation: Gong, Y.-N.; Ma, Q.-Y.; Wang, Y.; Zhang, J.-H.; Zhang, Y.-P.; Liang, R.-X.; Wang, B.-J.; Xie, S.-M.; Yuan, L.-M. Preparation of Chiral Porous Organic Cage Clicked Chiral Stationary Phase for HPLC Enantioseparation. *Molecules* **2023**, *28*, 3235. <https://doi.org/10.3390/molecules28073235>

Academic Editor: Harish Kumar Chopra

Received: 6 March 2023
Revised: 2 April 2023
Accepted: 3 April 2023
Published: 4 April 2023



Copyright: © 2023 by the authors. Licensee MDPI, Basel, Switzerland. This article is an open access article distributed under the terms and conditions of the Creative Commons Attribution (CC BY) license (<https://creativecommons.org/licenses/by/4.0/>).

1. Introduction

Many chemical molecules are chiral. There are two or more enantiomers of one chiral molecule. The resolution of chiral compounds is very important in many fields, particularly in pharmaceutical manufacturing because different enantiomers of a chiral pharmaceutical have different biological, pharmacological, and toxicological effects in organisms [1,2]. However, the resolution of enantiomers is also a challenging task due to their identical non-optical physicochemical properties. Among the many chiral separation methods reported to date, high-performance liquid chromatography (HPLC) using various chiral stationary phases (CSPs) has been proven to be an effective approach for chiral separation due to its advantages of high separation efficiency and wide range of application [3–7]. The enantioselectivity of the CSP is key to this approach. At present, a lot of CSPs have been employed for HPLC enantioseparation, such as polysaccharides [4,6,8], cinchona alkaloids [9,10], chiral crown ethers [11], cyclodextrins [12–14], and macrocyclic antibiotics [15,16]. However, most CSPs have some drawbacks, such as limited enantioselectivity and high production cost. Hence, the development of versatile CSPs with exceptional performance has always been a hot topic in chiral separation research.

The use of novel porous materials including metal-organic frameworks (MOFs) [17–19], covalent organic frameworks (COFs) [20–23], and porous organic polymers (POPs) [24,25]

as chromatographic stationary phases for separations has attracted a lot of research interest in recent years. These porous materials exhibit good separation performance due to their peculiar characteristics, such as high specific surface areas, defined pore structures, controllable pore sizes, and diverse topological structures. In general, such porous materials are expanded to frameworks or networks via strong covalent bonds or coordination bonds. Therefore, they are insoluble and inconvenient for chemical modification, coating, and immobilization on a chromatographic matrix, which will affect the preparation of efficient chromatographic columns or stationary phases. For instance, when they serve as selectors for the preparation of capillary columns or HPLC stationary phases, their particle suspensions are usually used for coating or bonding onto the inner wall of the column or chromatographic matrix, rather than using homogeneous solutions, which undoubtedly affects the column preparation, column efficiency, reproducibility, separation performance, etc. Porous organic cages (POCs) are a novel subclass of porous materials, which are composed of discrete, cage-like molecules with intrinsic cavities. The discrete molecules assemble into porous solids via weak intermolecular interactions instead of strong covalent bonds or coordination bonds [26–28]. When compared to the above-mentioned porous frameworks or networks (MOFs, COFs, and POPs), the most important characteristic of POCs is their good solubility, which enables them to have good solution processability. POCs have widely developed applications, including gas adsorption and storage [29–31], catalysis [32–34], separation [35–37], sensing [38–40], and bioimaging [41,42]. The development of POCs as CSPs for chromatographic chiral separation has also received a great deal of attention. In recent years, our group previously reported many chiral POCs as CSPs for gas chromatography (GC) chiral separation with good enantioselectivity [43–47]. More recently, a chiral POC NC1-R used as a selector to prepare CSP for HPLC enantioseparation has also been reported by our group, which demonstrates the potential application of POCs in HPLC [48]. Nevertheless, the utilization of chiral POCs for HPLC enantioseparation is still at a very early stage. Thus, the exploration of more and more chiral POCs with different geometrical structures, pore channels, window sizes, and cavities for the preparation of CSPs for HPLC is of great significance.

Click chemistry is a synthetic concept, which was first proposed by Sharpless in 2001 [49]. The aim of click chemistry is to rapidly and reliably accomplish the chemical synthesis of target molecules via the concatenation of small units. Click chemistry has been extensively used in many fields due to its merits of high reaction efficiency, mild conditions, high selectivity, and low by-products formation. Click reaction has also been widely used to prepare chromatographic stationary phases, such as thiol-ene click reaction and azide-alkyne click reaction [10,11,50]. Herein, we report the use of a [4 + 6]-type chiral POC as a selector to prepare a CSP using a thiol-ene click reaction to separate racemates and positional isomers in HPLC. The chiral POC ($C_{120}H_{96}N_{12}O_4$) was synthesized via the Schiff-base condensation of 2-hydroxy-1,3,5-benzenetri-aldehyde with (1*R*, 2*R*)-1,2-diphenyl-1,2-ethylenediamine [51], which was clicked onto thiol-functionalized silica gel to prepare the CSP. The CSP packed column showed good selectivity toward various racemates and disubstituted benzene isomers. The influence of the injection mass and column temperature on the separation, repeatability, and stability of the column have been explored.

2. Results and Discussion

2.1. Characterization of the Prepared Chiral POC and CSP

A variety of methods were used to characterize the chiral POC and CSP, including FT-IR, MALDI-TOF MS, NMR, TGA, and elemental analyses. From the FT-IR spectrum (Figure 1a), we can see the sharp and strong absorption at 1636 cm^{-1} was attributed to the imine bonds ($-C=N-$) in the chiral POC. The absorption at 3420 cm^{-1} represents the stretching vibration of phenolic hydroxyl ($-OH$), and the absorption peaks at 3062 and 2866 cm^{-1} can be ascribed to $N=C-H$ and saturated $C-H$ stretching vibrations, respectively. In addition, absorption bands at 3031 , 1600 , 1490 , and 1456 cm^{-1} are the characteristic absorption peaks of the benzene ring. The molecular weight computed from the molecular formula of the chiral POC

($C_{120}H_{96}N_{12}O_4$) is 1769.77. MALDI-TOF-MS (Figure 1b) exhibits peaks at $m/z = 1770.70$ and 885.86, which correspond to the ions peaks of $[M + H]^+$ and $[M + 2H]^{2+}$, respectively. The contents of C, H, and N calculated from the molecular formula ($C_{120}H_{96}N_{12}O_4$) are C 81.42%, H 5.47%, and N 9.50%; our elemental analysis found C 81.13%, H 5.36%, and N 9.52%. The NMR data of POC: 1H NMR (500 MHz, $CDCl_3$, ppm) δ : 14.51–14.22 (ddd, 4H), 8.90–8.84 (m, 4H), 8.66–8.58 (m, 4H), 8.40–8.37 (m, 4H), 8.30–8.17 (m, 8H), 7.22–7.06 (m, 6H), 4.86–4.66 (m, 12H). All of our characterization data fully support the successful synthesis of the chiral POC.

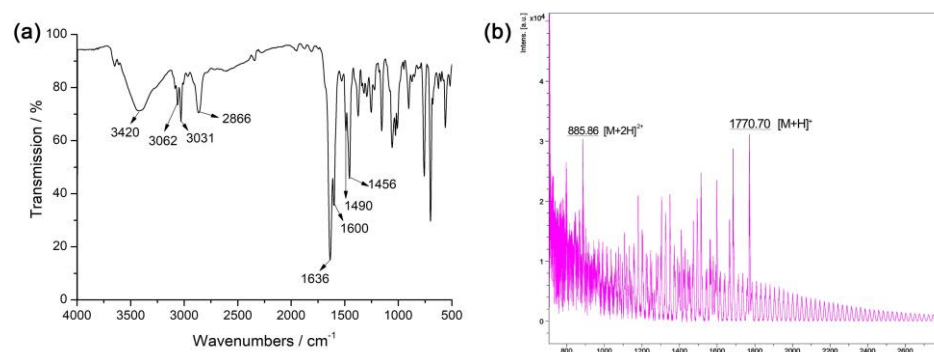


Figure 1. (a) FT-IR and (b) MALDI-TOF-MS spectra obtained for the chiral POC.

The fourier transform infrared spectra obtained for the thiol-functionalized silica gel (SiO_2-SH), CSP and chiral POC are shown in Figure 2a. When compared with SiO_2-SH , the intensity of the absorption peaks was obviously strengthened at 1636 and 2866 cm^{-1} , and new absorption peaks appeared at 1490 and 1456 cm^{-1} in the CSP, indicating that the POC cage molecules were successfully bonded onto the surface of SiO_2-SH . The TGA curves (Figure 2b) show that, when compared with SiO_2-SH , the weight of the CSP decreased significantly, further demonstrating that the chiral POC was attached to the surface of SiO_2-SH . Moreover, the elemental analyses of the C, H, and N content in SiO_2 , SiO_2-SH , and CSP are shown in Table S1. The C, H, and N contents in the CSP were obviously higher than those in SiO_2-SH , which also proved the successful binding of the chiral POC onto SiO_2-SH . The surface-bound quantity of the chiral POC onto SiO_2-SH was determined to be 0.18 $\mu mol m^{-2}$ according to Equation (1) (see Section 3.6).

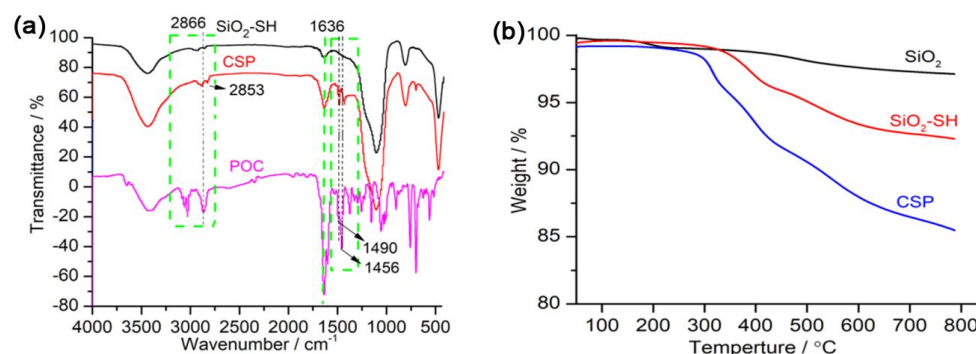


Figure 2. (a) FT-IR spectra obtained for the prepared chiral POC, SiO_2-SH , and CSP. (b) TGA curves of the SiO_2 , SiO_2-SH , and CSP.

2.2. Resolution of Racemates

To evaluate the chiral separation performance of the CSP, some chiral compounds were separated on the packed column using different proportions of *n*-hexane/isopropanol as the mobile phase. Thirteen racemic compounds were resolved on the column, including alcohols, diols, organic acids, ketones, amines, and epoxides. The chromatographic data obtained for the resolved racemates including the retention factor (k_1), separation factor (α),

and resolution (R_s), were calculated and shown in Table 1. The resulting chromatograms are presented in Figure 3. Table 1 and Figure 3 show that this column exhibits good separation performance for some racemic mixtures, which have high R_s values, for instance, the resolution of 1-(1-naphthyl)ethanol ($R_s = 4.10$), 3-benzyloxy-1,2-propanediol ($R_s = 3.45$), 2-phenyl-1-propanol ($R_s = 2.30$), 1-phenylethylamine ($R_s = 3.72$), and ofloxacin ($R_s = 6.95$), demonstrating the good enantioselectivity of the CSP.

Table 1. Resolution of racemates on the chiral POC NC1-R-based column, Chiralpak AD-H, and Chiralcel OD-H columns.

Racemates	This Column			NC1-R Column [48]			Chiralpak AD-H Column			Chiralcel OD-H Column		
	k_1	α	R_s	k_1	α	R_s	k_1	α	R_s	k_1	α	R_s
1-(1-Naphthyl)ethanol ^a	1.11	4.80	4.10	1.28	2.09	4.09	1.47	1.00	– ^d	1.93	1.14	1.23
3-Benzyloxy-1,2-propanediol ^a	1.63	1.87	3.45	4.65	1.63	5.47	2.24	1.19	0.70	2.73	1.06	2.12
2-Phenyl-1-propanol ^b	1.27	1.62	2.30	1.10	1.00	– ^d	1.36	1.00	– ^d	1.52	1.16	1.82
<i>trans</i> -1,2-Diphenylethylene oxide ^a	1.17	1.47	1.38	0.54	1.33	0.74	0.86	2.76	19.8	0.83	1.95	4.38
Benzoin ^a	1.67	1.46	1.31	3.41	1.08	1.26	4.70	1.36	6.96	2.52	1.58	6.53
1-Phenyl-1-propanol ^a	1.14	1.47	1.38	1.04	1.50	2.04	0.83	1.06	0.63	0.83	1.11	0.50
Hydrobenzoin ^a	1.22	1.62	1.81	0.76	1.57	2.50	0.36	1.00	– ^d	2.62	1.00	– ^d
1-Phenylethylamine ^c	1.41	1.90	3.72	0.86	1.37	1.88	0.71	1.00	– ^d	0.96	1.19	0.81
Ofloxacin ^d	1.01	3.45	6.95	0.92	1.00	– ^d	0.55	1.00	– ^d	0.90	1.00	– ^d
Mandelic acid ^a	1.52	1.41	1.02	0.77	1.73	3.13	3.36	1.20	4.55	2.20	1.06	0.62
Naproxen ^a	2.20	1.81	1.33	2.01	1.00	– ^d	3.10	1.00	– ^d	1.07	1.00	– ^d
1-(4-Chlorophenyl)ethanol ^a	1.49	1.17	1.12	1.13	1.51	3.07	0.86	1.04	0.49	0.78	1.13	0.67
1-(3-Methylphenyl)ethanol ^a	1.58	1.11	0.34	1.08	1.00	– ^d	0.93	1.00	– ^d	0.75	1.25	1.26

Experimental conditions: column temperature, 25 °C; flow rate, 0.1 mL min^{−1}. ^a Mobile phase: *n*-hexane/isopropanol = 90/10 (*v/v*); ^b mobile phase: *n*-hexane/isopropanol = 85/15 (*v/v*); ^c mobile phase: *n*-hexane/isopropanol = 95/5 (*v/v*); *n*-hexane/isopropanol = 99/1 (*v/v*); ^d: could not be separated.

The 13 chiral compounds tested were also separated on a previously reported chiral POC NC1-R-based CSP packed column, Chiralpak AD-H, and Chiralcel OD-H columns for comparison (Table 1). There are 4 racemates, namely 2-phenyl-1-propanol, ofloxacin, naproxen, and 1-(3-methylphenyl)ethanol, which cannot be separated on the NC1-R-based CSP packed column (Table 1). In addition, some racemates cannot be separated on the Chiralpak AD-H and Chiralcel OD-H columns, while they can be well separated on this column: 1-(1-naphthyl)ethanol, hydrobenzoin, 1-phenylethylamine, ofloxacin, and naproxen cannot be separated on the Chiralpak AD-H column; hydrobenzoin, ofloxacin, mandelic acid, and naproxen cannot be separated on the Chiralcel OD-H column. Moreover, some racemates can be separated on this column with higher R_s and α values than on the NC1-R, Chiralpak AD-H, and Chiralcel OD-H columns (Table 1). Some of the chromatograms obtained on these columns are compared in Figure S3. The results indicate that this column can be complementary to the previously reported chiral POC NC1-R, Chiralpak AD-H, and Chiralcel OD-H columns in terms of enantiomeric separation, which can separate some chiral compounds that cannot be separated using the three columns.

The good chiral resolution ability of the CSP was well correlated with the molecular structure of the chiral POC. The synthesized chiral POC molecule has a tetrahedral structure and subtriangular pore windows on each face (Figure S4). The discrete cage molecules are packed into the porous solid via weak intermolecular forces. Due to the enantiomerically pure (1*R*, 2*R*)-1,2-diphenyl-1,2-ethylenediamine serving as one building unit, each molecule of the POC is chiral. Figure S4a shows there is an internal cavity in each molecular center. Analytes can access the cavity through the pore window and abundant host-guest interactions will occur. For example, the CSP offers good enantioselectivity for the separation of chiral alcohols, in which hydrogen bonding interactions formed between the hydroxyl groups of the racemates and N, and O atoms of the chiral POC probably play an important role. In addition, other interactions formed between the chiral POC molecule

and analytes, such as dipole-dipole, π - π , and van der Waals interactions, are also crucial for chiral separation. Overall, the good enantioselectivity of the chiral POC-based CSP results from its unique molecular structure (i.e., internal cavity and cage-like molecular structure), by which host-guest inclusion, hydrogen bonding, dipole-dipole, π - π , and van der Waals interactions play crucial roles in the chiral separation.

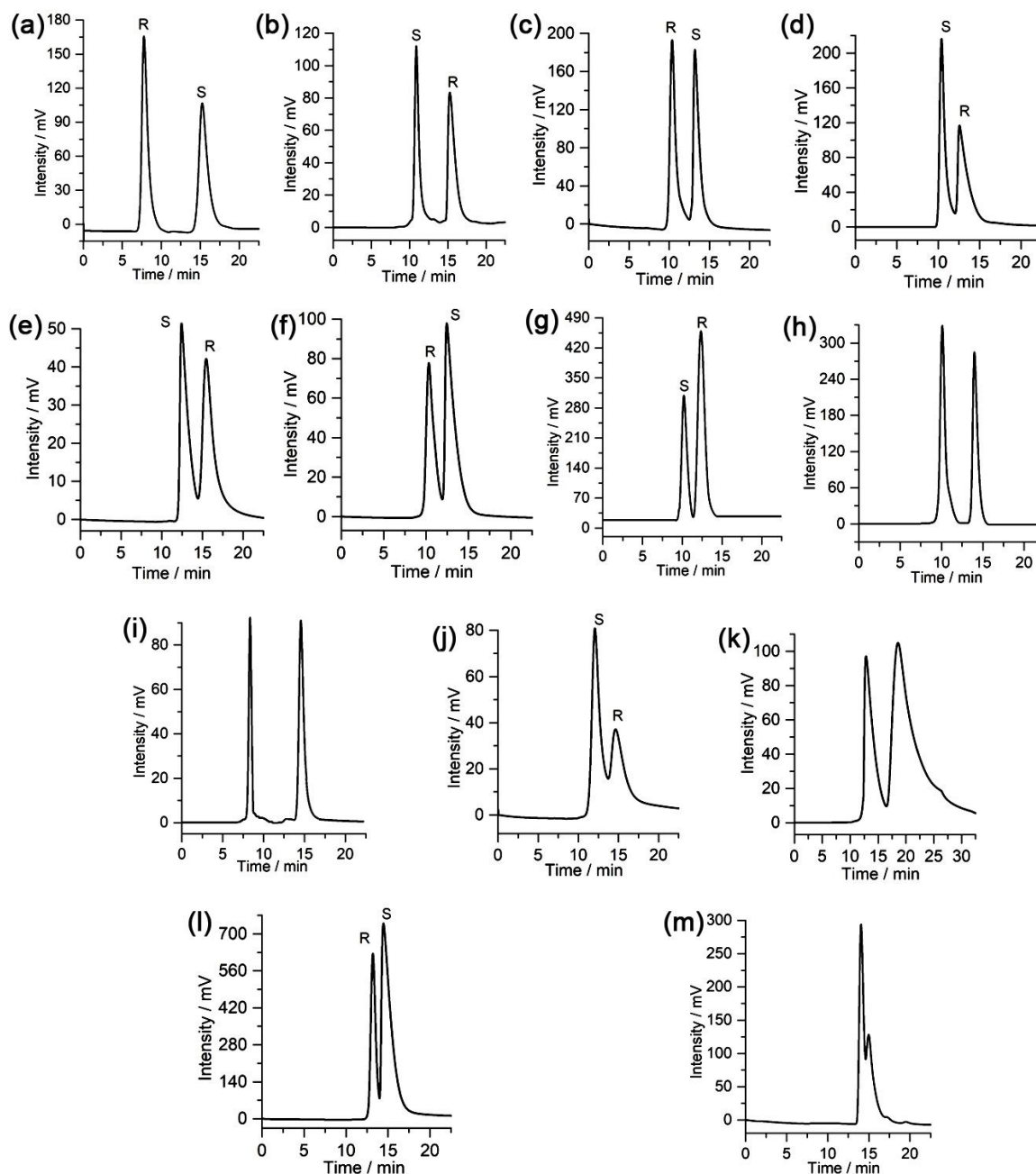


Figure 3. Chromatograms obtained for the separation of racemates on the chiral POC-based CSP packed column: (a) 1-(1-Naphthyl)ethanol, (b) 3-benzyloxy-1,2-propanediol, (c) 2-phenyl-1-propanol, (d) *trans*-1,2-diphenylethylene oxide, (e) benzoin, (f) 1-phenyl-1-propanol, (g) hydrobenzoin, (h) 1-phenylethylamine, (i) ofloxacin, (j) mandelic acid, (k) naproxen, (l) 1-(4-chlorophenyl)ethanol, and (m) 1-(3-methylphenyl)ethanol.

2.3. Separation of Positional Isomers

Disubstituted benzene isomers have important applications in industrial production and each positional isomer has unique applications. Therefore, the separation of such

positional isomers is particularly important. Nevertheless, positional isomers are difficult to separate due to their analogous physicochemical properties, such as functional groups, boiling point, and dimensions. The CSP also shows a good separation performance toward some disubstituted benzene isomers. Table 2 and Figure 4 show that eight positional isomers (iodoaniline, bromoaniline, chloroaniline, dibromobenzene, dichlorobenzene, toluidine, nitrobromobenzene, and nitroaniline) have been separated on this column. Some positional isomers were separated with higher resolution values, such as the separation of *o*-/*m*-iodoaniline ($R_s = 3.26$), *o*-/*m*-bromoaniline ($R_s = 3.82$), *m*-/*o*-dibromobenzene ($R_s = 8.03$), and *m*-/*o*-dichlorobenzene ($R_s = 9.66$). Our results show that the CSP has a good separation capability toward positional isomers and certain application prospects.

Table 2. Separation of positional isomers on the chiral POC column.

Positional Isomers	Separation Factor (α)		Resolution (R_s)	
	α_1	α_2	R_{s1}	R_{s2}
Iodoaniline ^a	2.17	1.25	3.26	1.52
Bromoaniline ^a	2.11	1.29	3.82	1.45
Chloroaniline ^a	2.05	1.31	2.95	1.31
Dibromobenzene ^a	1.21	2.54	1.42	8.03
Dichlorobenzene ^a	1.17	3.02	1.31	9.66
Toluidine ^a	1.25	1.44	1.60	1.77
Nitrobromobenzene ^b	1.32	1.84	1.58	1.90
Nitroaniline ^a	1.37	1.84	1.74	0.89

Experimental conditions: column temperature, 25 °C; flow rate, 0.1 mL min⁻¹. ^a Mobile phase: *n*-hexane/isopropanol = 90/10 (*v/v*); ^b mobile phase: *n*-hexane/isopropanol = 99/1 (*v/v*).

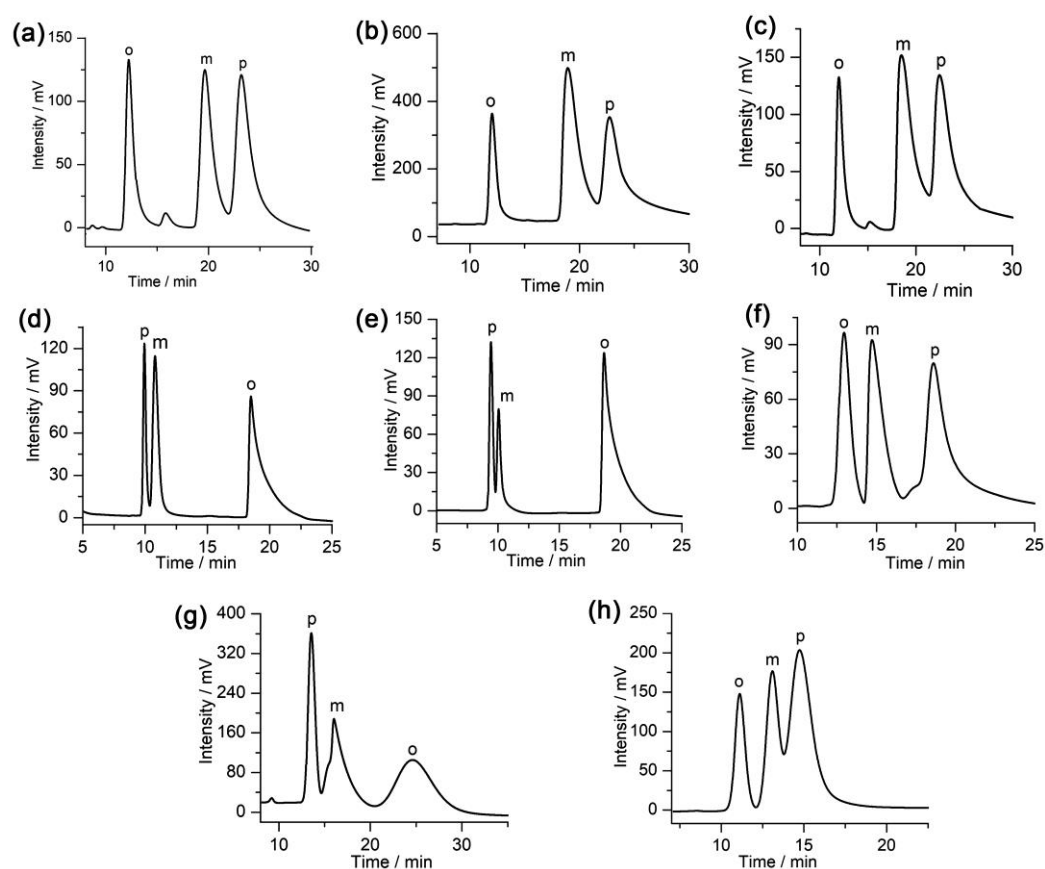


Figure 4. Chromatograms obtained for the separation of positional isomers on the chiral POC-based CSP packed column: (a) iodoaniline, (b) bromoaniline, (c) chloroaniline, (d) dibromobenzene, (e) dichlorobenzene, (f) toluidine, (g) nitrobromobenzene, and (h) nitroaniline.

2.4. Effect of Injection Mass on Separation

In order to investigate the effect of the injection amount on the separation, various amounts (from 1 to 20 μg) of racemic hydrobenzoin and isomeric iodoaniline were injected into the column. The obtained chromatograms are presented in Figure 5. The results show that the chromatographic peak area increases linearly with an increase in the injection amount (Figure 5), whereas the retention times were almost unchanged. At the same time, the half-peak width increases with an increase in the injection amount and the selectivity decreased (Figure 5). Therefore, an appropriate injection amount should be selected during the separation and analysis of the samples. To achieve better separation effects, the injection mass of hydrobenzoin and iodoaniline should not exceed 10 μg and 5 μg , respectively.

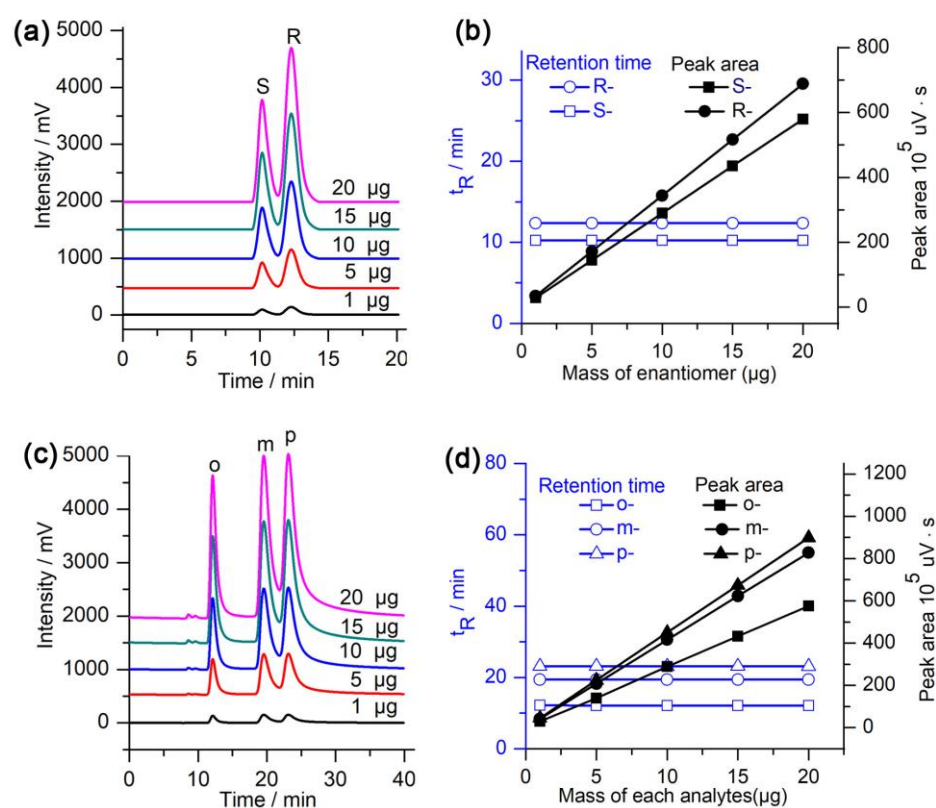


Figure 5. Effect of the injection amount on the separation: (a,c) Chromatograms obtained for with various amounts of hydrobenzoin and iodoaniline and (b,d) effect of various amounts of hydrobenzoin and iodoaniline on the retention time and peak area. Other chromatographic conditions are the same as those in Tables 1 and 2.

2.5. Effect of the Column Temperature on Separation

To evaluate the effect of the column temperature on separation, racemic hydrobenzoin and isomeric iodoaniline were injected into the column and separated using a column temperature in the range of 20–45 $^{\circ}\text{C}$. It can be seen from Figure 6 that the retention time of hydrobenzoin and iodoaniline on the column decreases as the temperature increases and the resolution value decreases accordingly, which indicates that the separations were exothermic processes.

The Van't Hoff curves obtained for hydrobenzoin and iodoaniline using this column at different column temperatures are shown in Figure 7. A good linear correlation between $\ln k'$ and $1/T$ demonstrates that the separation mechanism did not change at the column temperatures studied. The Gibbs free energy change (ΔG), enthalpy change (ΔH), and entropy change (ΔS) of the analytes were calculated and shown in Table 3 (see Section 3.7 for the computation formula used for ΔG , ΔH , and ΔS). Table 3 shows the ΔG values of *R,R*-/*S,S*-hydrobenzoin and *o*, *m*, *p*-iodoaniline were negative, indicating that the transfer of the samples

from the mobile phase to the CSP was a thermodynamically spontaneous process. The more negative ΔG of the analyte, the easier it transfers from the mobile phase to the CSP, which will result in a longer retention time. Table 3 shows $\Delta G_{(R,R\text{-hydrobenzoin})} < \Delta G_{(S,S\text{-hydrobenzoin})}$ and $\Delta G_{(p\text{-iodoaniline})} < \Delta G_{(m\text{-iodoaniline})} < \Delta G_{(o\text{-iodoaniline})}$. Theoretically, the retention time sequence was $R,R\text{-hydrobenzoin} > S,S\text{-hydrobenzoin}$ and $p\text{-iodoaniline} > m\text{-iodoaniline} > o\text{-iodoaniline}$, which was in accordance with the chromatograms (Figure 6).

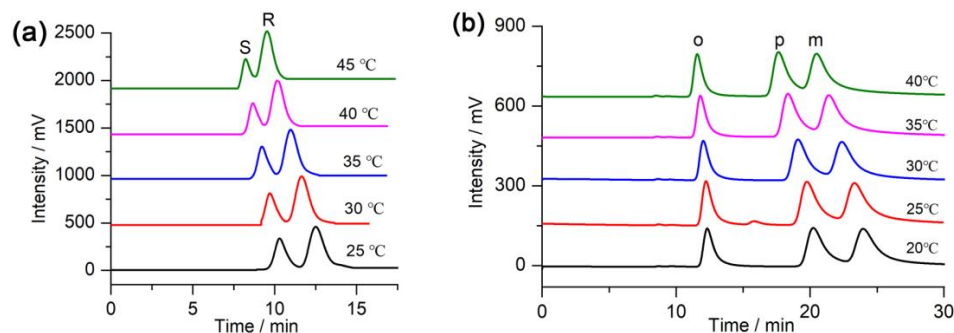


Figure 6. Separation of (a) hydrobenzoin and (b) iodoaniline on the column at different column temperatures. The other chromatographic conditions are the same as those in Tables 1 and 2.

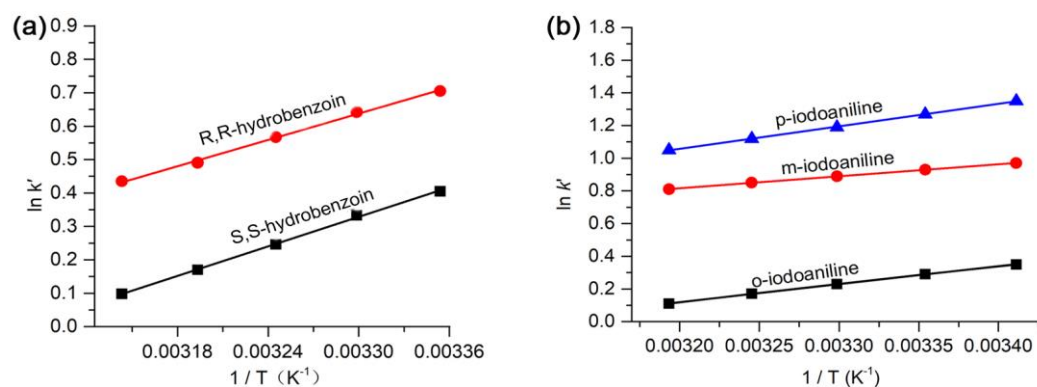


Figure 7. Van't Hoff curves obtained for (a) hydrobenzoin and (b) iodoaniline.

Table 3. ΔH , ΔS , ΔG and correlation coefficient (R^2) values for the separation of hydrobenzoin and iodoaniline.

Analytes	ΔH (kJ mol ⁻¹)	ΔS (J mol ⁻¹ K ⁻¹)	ΔG (kJ mol ⁻¹)	R^2
S,S-Hydrobenzoin	-10.91 ± 0.31	-31.62 ± 0.99	-1.48 ± 0.31	0.9987
R,R-Hydrobenzoin	-12.25 ± 0.22	-35.60 ± 0.72	-1.64 ± 0.22	0.9968
<i>o</i> -Iodoaniline	-6.41 ± 0.10	-20.18 ± 0.34	-3.53 ± 0.10	0.9986
<i>m</i> -Iodoaniline	-9.14 ± 0.07	-4.16 ± 0.22	-4.87 ± 0.07	0.9986
<i>p</i> -Iodoaniline	-11.23 ± 0.11	-5.64 ± 0.38	-10.79 ± 0.11	0.9974

2.6. Reproducibility and Stability of the Column

The excellent stability and reproducibility of a chromatographic column are important for its practical application. To study the reproducibility and stability of the column, the separation of hydrobenzoin and iodoaniline was performed after different times of injection. Figure S5 shows the chromatograms obtained for hydrobenzoin and iodoaniline on the column after it has undergone 10, 100, 200, and 300 injections. Figure S5 shows there are no significant changes in the retention times and selectivities, and the relative standard deviations (RSDs) were $<1.0\%$ and $<1.5\%$ for the retention time and selectivity, respectively, demonstrating that this column has good repeatability and stability for separation.

3. Materials and Methods

3.1. Chemicals and Reagents

Phenol, (1*R*, 2*R*)-1,2-diphenyl-1,2-ethanediamine, hexamethylenetetramine (HMTA), 1-allylimidazole, 1,4-dibromobutane, azodiisobutyronitrile (AIBN), (3-mercaptopropyl) trimethoxysilane, trifluoroacetic acid (TFA) and K_2CO_3 were obtained from Adamas-beta (Shanghai, China). Commercial spherical silica ($5\ \mu\text{m}$, $300\ \text{m}^2\ \text{g}^{-1}$) was provided from Suzhou Nanwei Technology Co., Ltd. (Suzhou, China). Other commonly used solvents, such as *N,N*-dimethylformamide (DMF), chloroform, toluene, acetonitrile, ethanol, and pyridine, were obtained from Tianjin Fengchuan Chemical Reagent Technology Co., Ltd. (Tianjin, China). Racemic 1-(3-methylphenyl) ethanol, 1-(1-naphthyl) ethanol, 1-(4-chlorophenyl) ethanol, mandelic acid, naproxen and ofloxacin were purchased from Adamas-beta (Shanghai, China); 2-phenyl-1-propanol, 3-benzyloxy-1,2-propanediol, hydrobenzoin, 1-phenyl-1-propanol, 1-phenylethylamine, benzoic acid, and *trans*-1,2-diphenylethylene oxide were obtained from Aladdin (Shanghai, China). Positional isomers, such as iodoaniline, bromoaniline, chloroaniline, dichlorobenzene, dibromobenzene, toluidine, nitroaniline, and nitrobenzene were provided from Adamas-beta (Shanghai, China).

3.2. Instrumentation

A Shimadzu LC-16 (Shimadzu, Kyoto, Japan) HPLC equipped with an SPD-16 UV-Vis detector and LC-16 pump was used in this work. A HPLC stainless-steel column ($250\ \text{mm} \times 2.1\ \text{mm}$ i.d.) and Alltech slurry packer (Alltech, Deerfield, IL, USA) were used for column packing. A Bruker DRX 500 spectrometer (Bruker, Bremen, Germany) was used to obtain the nuclear magnetic resonance (NMR) spectra. An SDT-650 thermal analyzer (TA Instruments, New Castle, DE, USA) was used to obtain the thermogravimetric analysis data. Mass spectrometry was carried out on a Bruker UltrafleXtreme MALDI-TOF mass spectrometer (Thermo Fisher, Bremen, Germany). Elemental analysis data were obtained on a Vario EL III elemental analyzer (Elementar, Langensfeld, Germany).

3.3. Synthesis of Chiral POC

The chiral POC was prepared according to the approach reported by M. Petryk et al. (Figure 8) [51]. The 2-hydroxy-1,3,5-benzenetri-aldehyde building block was first synthesized (see Supplementary Materials). (1*R*, 2*R*)-1,2-Diphenyl-1,2-ethanediamine (0.64 g, 3 mmol) was dissolved in 160 mL of $H_2O/DMSO$ (90/10, *v/v*) upon stirring. After 5 min, 2-hydroxy-1,3,5-benzenetri-aldehyde (0.36 g, 2 mmol) and TFA (15 μL) were added, and the resulting mixture was stirred at room temperature for 14 days. A yellow solid was generated during the reaction process. The mixture was filtered and the solid washed three times with chloroform and H_2O , and then dried at $70\ ^\circ\text{C}$ under vacuum for 6 h. Finally, the solid was recrystallized via slow diffusion of diethyl ether into a solution of the crude product in chloroform to afford the pure POC crystals (0.30 g, yield 35%).

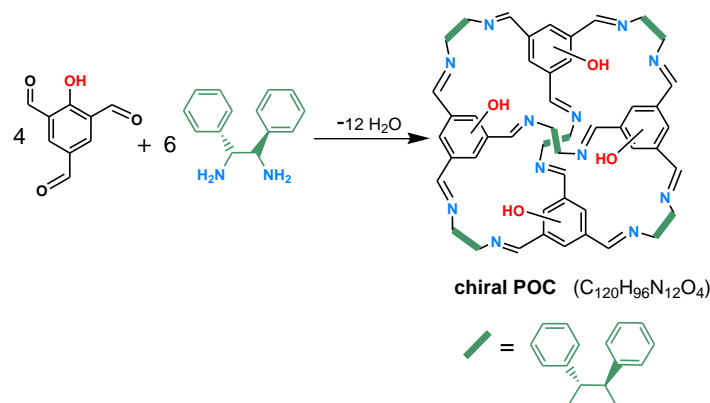


Figure 8. Synthesis of the chiral POC.

3.4. Preparation of the Chiral POC-Based CSP

Preparation of the CSP was carried out following the procedure described in Figure 9. The chiral POC was reacted with 1,4-dibromobutane and 1-allylimidazole to synthesize the alkenyl-functionalized chiral POC. The alkenyl-functionalized products were then attached to the thiol-functionalized silica gel using a thiol-ene click reaction. The detailed preparation process of the CSP was as follows:

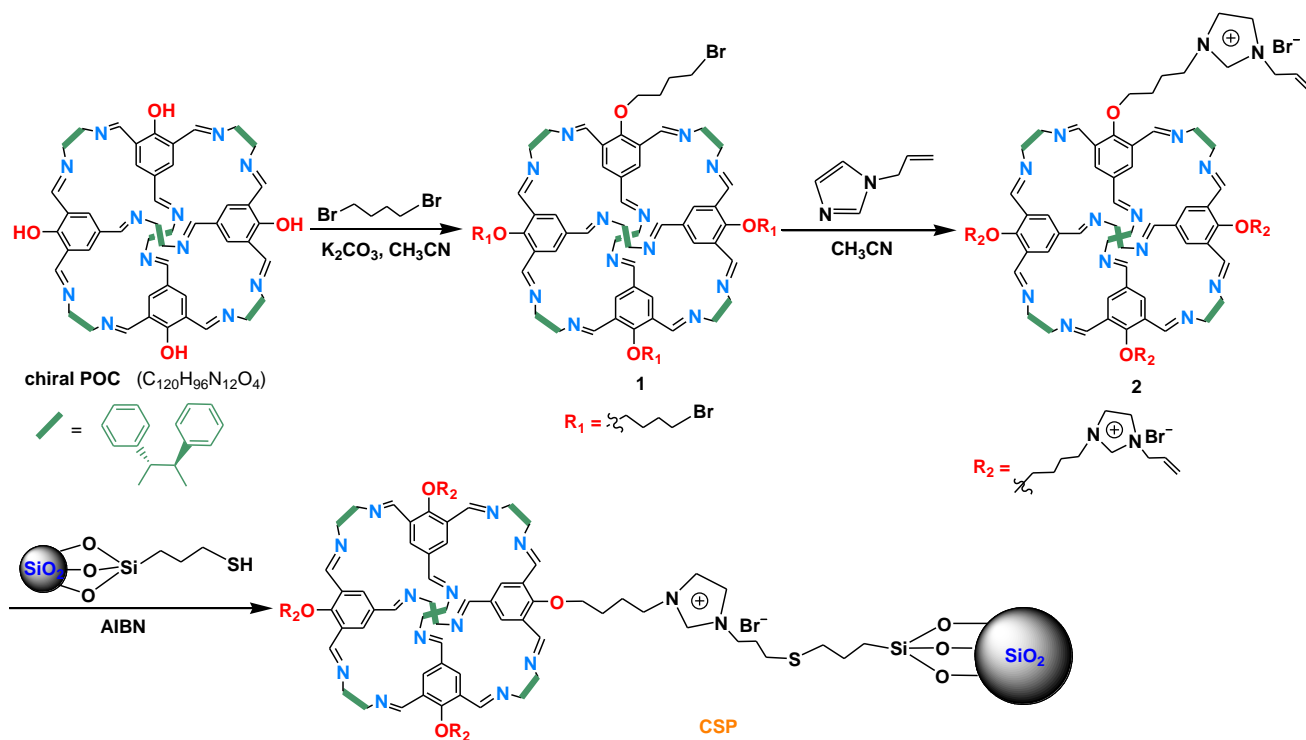


Figure 9. Preparation of the CSP.

3.4.1. Preparation of Thiol-Functionalized Silica Gel

Commercial spherical silica (5.0 g) was added to a 10% HCl solution, and the resulting mixture was stirred at 100 °C for 24 h. The resulting mixture was filtered and washed to neutral with deionized water, and then dried under vacuum at 180 °C to afford activated silica gel.

Activated silica (2.5 g) was dispersed in 50 mL of anhydrous toluene, and (3-mercaptopropyl)trimethoxysilane (2.0 mL) and anhydrous pyridine (0.5 mL) were then successively added. The resulting mixture was heated at reflux under the protection of an N₂ atmosphere. After 48 h, the reaction mixture was filtered and the resulting solid was washed with toluene, methanol, and acetone in sequence. The solid was then dried at 100 °C under vacuum for 6 h to obtain thiol-functionalized silica gel.

3.4.2. Synthesis of Alkenyl-Functionalized Chiral POC

Typically, a 250 mL round-bottom flask was charged with the synthesized chiral POC (0.5 g, 0.28 mmol) and potassium carbonate (0.2 g, 1.7 mmol), and 40 mL of acetonitrile was then added. After stirring for 5 min, 1,4-dibromobutane (0.2 mL) was added and the resulting mixture was heated at reflux for 48 h. The mixture was filtered, and the filtrate was concentrated in vacuo on a rotary evaporator to obtain a brown solid. The crude product was repeatedly washed with *n*-hexane and ultrapure water, and then dried at 80 °C under vacuum to obtain compound **1** (0.56 g).

Compound **1** (0.54 g) was dispersed in acetonitrile (60 mL) with the aid of ultrasound for 10 min, and 1-allylimidazole (0.3 mL) was then added. Subsequently, the reaction mixture was heated at 60 °C under a N₂ atmosphere for 48 h. The resulting solution was

concentrated to ~20 mL and then poured into *n*-hexane (20 mL) to form a precipitate. The solids were collected by filtration and washed with *n*-hexane, ultrapure water, and acetone, and then dried at 60 °C under vacuum to yield the alkenyl-functionalized chiral POC (compound 2) (0.58 g).

3.4.3. Bonding of Alkenyl-Functionalized Chiral POC onto Thiol-Functionalized Silica Gel

The alkenyl-functionalized chiral POC (compound 2, 0.54 g) and methanol (40 mL) were charged into a 100 mL round-bottom flask with stirring. After 30 min, thiol-functionalized silica gel (1.3 g) and AIBN (50 mg) were added, and then heated at 65 °C under a N₂ atmosphere. After reaction for 48 h, the resulting mixture was filtered, and the solid was washed with methanol and acetone. Finally, the solid was dried at 80 °C under vacuum to give the CSP.

3.5. Column Packing

The prepared CSP was packed into a HPLC stainless steel column using a slurry-packing technique. Firstly, the CSP (1.2 g) was uniformly dispersed in 20 mL of *n*-hexane/isopropanol (90/10, *v/v*). Then, using *n*-hexane/isopropanol (90/10, *v/v*) as the driving solvent, the suspensions was packed into the HPLC column using a slurry packer at a pressure of 30 MPa for 30 min.

3.6. Calculation of the Surface-Bound Amount of the CSP

The surface-bound amount of the chiral POC on the CSP was calculated according to the following formula (Equation (1)) [12,52]:

$$\frac{\mu\text{mol}}{\text{m}^2} = \frac{C\% \times 10^6}{S \times 12.001 \times N_c \times \left(100 - \frac{C\%}{N_c \times 12.001} \times M_r\right)} \quad (1)$$

where *C%* represents the increased carbon content compared to the thiol-functionalized silica gel, *N_c* represents the number of carbon atoms in the bonding portion, *M_r* represents the molecular weight of the bonding portion, and *S* represents the surface area of silica gel (300 m² g⁻¹).

3.7. Calculation of the Thermodynamic Parameters

The enthalpy change (ΔH), entropy change (ΔS), and Gibbs free energy change (ΔG) were calculated according to the following equations (Equations (2) and (3)) [53]:

$$\ln k' = -\frac{\Delta H}{RT} + \frac{\Delta S}{R} + \ln \Phi \quad (2)$$

$$\Delta G = \Delta H - T\Delta S \quad (3)$$

where *k'* is the retention factor, *R* is the gas constant, *T* is the absolute temperature, and Φ is the phase ratio. *k'* was calculated according to (Equation (4)).

$$k' = \frac{t_R - t_0}{t_0} \quad (4)$$

where *t_R* is the retention time of the enantiomers and *t₀* is the dead time.

4. Conclusions

We have prepared a POC-based chiral CSP for HPLC separations. The experimental results demonstrate that the column allows to achieve a good separation of some racemic compounds and positional isomers. Thirteen racemic compounds belonging to various classes and eight positional isomers were separated on the CSP packed column. The column can be complementary to the previously reported chiral POC NC1-R-based column, Chiralpak AD-H and Chiralcel OD-H columns in terms of their enantioseparation, and can

separate some racemates that cannot be separated using the three previously reported chromatographic columns. In addition, the column exhibited good stability and repeatability for separation after multiple injections. This work indicates that POC has great potential in HPLC separation.

Supplementary Materials: The following supporting information can be downloaded at: <https://www.mdpi.com/article/10.3390/molecules28073235/s1>, Figure S1: Preparation of 2-hydroxy-1,3,5-benzenetri-aldehyde; Figure S2: The NMR spectra of 2-hydroxy-1,3,5-benzenetri-aldehyde; Figure S3: Comparison of the separation of some racemates on this POC-based column, Chiralcel AD-H column, and Chiralpak OD-H column. Figure S4: (a) Structure of the chiral POC molecule; (b) Shape of the pore window on each face; Figure S5: Chromatograms for the separation of (a) hydrobenzoin and (b) iodoaniline after the column were subjected to different injection times; Table S1: The results of elemental analysis of SiO₂-SH and CSP. Reference [54] is cited in the Supplementary Materials.

Author Contributions: Conceptualization, Y.-N.G. and J.-H.Z.; methodology, Y.W. and Q.-Y.M.; software, B.-J.W., Q.-Y.M. and Y.-P.Z.; validation, R.-X.L. and S.-M.X.; formal analysis, Y.-P.Z. and Y.W.; investigation, Y.-N.G., Q.-Y.M. and Y.W.; resources, J.-H.Z., B.-J.W., S.-M.X. and L.-M.Y.; data curation, R.-X.L.; writing-original draft preparation, Y.-N.G. and Y.W.; writing-review and editing, Y.-N.G. and J.-H.Z.; supervision, J.-H.Z. and B.-J.W.; project administration, J.-H.Z.; funding acquisition, J.-H.Z., B.-J.W., S.-M.X. and L.-M.Y. All authors have read and agreed to the published version of the manuscript.

Funding: This work was supported by the National Natural Science Foundation of China (Nos. 22064020, 21964021, and 22174125) and the Applied Basic Research Foundation of Yunnan Province (Nos. 202101AT070101, and 202201AT070029).

Institutional Review Board Statement: Not applicable.

Informed Consent Statement: Not applicable.

Data Availability Statement: All relevant data are included in the article.

Conflicts of Interest: The authors declare no conflict of interest.

Sample Availability: Samples of the compounds are not available from the authors.

References

1. Wang, R.Q.; Ong, T.T.; Ng, S.C.; Tang, W.H. Recent advances in pharmaceutical separations with supercritical fluid chromatography using chiral stationary phases. *TrAC-Trends Anal. Chem.* **2012**, *37*, 83–100.
2. Maier, N.M.; Franco, P.; Lindner, W. Separation of enantiomers: Needs, challenges, perspectives. *J. Chromatogr. A* **2001**, *906*, 3–33. [[CrossRef](#)] [[PubMed](#)]
3. Shen, J.; Okamoto, Y. Efficient separation of enantiomers using stereoregular chiral polymers. *Chem. Rev.* **2016**, *116*, 1094–1138. [[CrossRef](#)] [[PubMed](#)]
4. Chankvetadze, B. Recent trends in preparation, investigation and application of polysaccharide-based chiral stationary phases for separation of enantiomers in high-performance liquid chromatography. *TrAC-Trends Anal. Chem.* **2020**, *122*, 115709. [[CrossRef](#)]
5. Lämmerhofer, M. Chiral recognition by enantioselective liquid chromatography: Mechanisms and modern chiral stationary phases. *J. Chromatogr. A* **2010**, *1217*, 814–856. [[CrossRef](#)] [[PubMed](#)]
6. Tang, S.; Mei, X.; Chen, W.; Huang, S.H.; Bai, Z.W. A high-performance chiral selector derived from chitosan (p-methylbenzylurea) for efficient enantiomer separation. *Talanta* **2018**, *185*, 42–52. [[CrossRef](#)]
7. Teixeira, J.; Tiritan, M.E.; Pinto, M.M.; Fernandes, C. Chiral stationary phases for liquid chromatography: Recent developments. *Molecules* **2019**, *24*, 865. [[CrossRef](#)] [[PubMed](#)]
8. Okamoto, Y.; Yashima, E. Polysaccharide derivatives for chromatographic separation of enantiomers. *Angew. Chem. Int. Ed.* **1998**, *37*, 1020–1043. [[CrossRef](#)]
9. Lämmerhofer, M.; Lindner, W. Quinine and quinidine derivatives as chiral selectors I. Brush type chiral stationary phases for high-performance liquid chromatography based on cinchonan carbamates and their application as chiral anion exchangers. *J. Chromatogr. A* **1996**, *741*, 33–48. [[CrossRef](#)]
10. Ferri, M.; Bäurer, S.; Carotti, A.; Wolter, M.; Alshaar, B.; Theiner, J.; Ikegami, T.; West, C.; Lämmerhofer, M. Fragment-based design of zwitterionic, strong cation- and weak anion-exchange type mixed-mode liquid chromatography ligands and their chromatographic exploration. *J. Chromatogr. A* **2020**, *1621*, 461075. [[CrossRef](#)]
11. Hyun, M.H. Liquid chromatographic enantioseparations on crown ether-based chiral stationary phases. *J. Chromatogr. A* **2016**, *1467*, 19–32. [[CrossRef](#)]

12. Yao, X.; Zheng, H.; Zhang, Y.; Ma, X.; Xiao, Y.; Wang, Y. Engineering thiol–ene click chemistry for the fabrication of novel structurally well-defined multifunctional cyclodextrin separation materials for enhanced enantioseparation. *Anal. Chem.* **2016**, *88*, 4955–4964. [[CrossRef](#)] [[PubMed](#)]
13. Wang, R.Q.; Ong, T.T.; Tang, W.; Ng, S.C. Cationic cyclodextrins chemically-bonded chiral stationary phases for high-performance liquid chromatography. *Anal. Chim. Acta* **2012**, *718*, 121–129. [[CrossRef](#)] [[PubMed](#)]
14. Li, H.; Wang, X.; Shi, C.; Zhao, L.; Li, Z.; Qiu, H. Chiral phenethylamine synergistic tricarboxylic acid modified β -cyclodextrin immobilized on porous silica for enantioseparation. *Chin. Chem. Lett.* **2022**, *34*, 107606. [[CrossRef](#)]
15. Armstrong, D.W.; Tang, Y.; Chen, S.; Zhou, Y.; Bagwill, C.; Chen, J.R. Macrocyclic antibiotics as a new class of chiral selectors for liquid chromatography. *Anal. Chem.* **1994**, *66*, 1473–1484. [[CrossRef](#)]
16. De Gauquier, P.; Vanommeslaeghe, K.; Vander Heyden, Y.; Mangelings, D. Modelling approaches for chiral chromatography on polysaccharide-based and macrocyclic antibiotic chiral selectors: A review. *Anal. Chim. Acta* **2022**, *1198*, 338861. [[CrossRef](#)] [[PubMed](#)]
17. Jiang, H.; Yang, K.; Zhao, X.; Zhang, W.; Liu, Y.; Jiang, J.; Cui, Y. Highly stable Zr(IV)-based metal–organic frameworks for chiral separation in reversed-phase liquid chromatography. *J. Am. Chem. Soc.* **2020**, *143*, 390–398. [[CrossRef](#)]
18. Meng, S.S.; Xu, M.; Han, T.; Gu, Y.H.; Gu, Z.Y. Regulating metal–organic frameworks as stationary phases and absorbents for analytical separations. *Anal. Methods* **2021**, *13*, 1318–1331. [[CrossRef](#)] [[PubMed](#)]
19. Yu, Y.; Xu, N.; Zhang, J.; Wang, B.; Xie, S.; Yuan, L. Chiral metal–organic framework d-His-ZIF-8@SiO₂ core–shell microspheres used for HPLC enantioseparations. *ACS Appl. Mater. Inter.* **2020**, *12*, 16903–16911. [[CrossRef](#)] [[PubMed](#)]
20. Qian, H.L.; Yang, C.X.; Yan, X.P. Bottom-up synthesis of chiral covalent organic frameworks and their bound capillaries for chiral separation. *Nat. Commun.* **2016**, *7*, 12104. [[CrossRef](#)] [[PubMed](#)]
21. Xie, M.; Quan, K.; Li, H.; Liu, B.; Chen, J.; Yu, Y.; Wang, J.; Qiu, H. Non-porous silica support covalent organic frameworks as stationary phases for liquid chromatography. *Chem. Commun.* **2022**, *59*, 314–317. [[CrossRef](#)] [[PubMed](#)]
22. Fu, Y.; Li, Z.; Li, Q.; Hu, C.; Liu, Y.; Sun, W.; Chen, Z. In situ room-temperature preparation of a covalent organic framework as stationary phase for high-efficiency capillary electrochromatographic separation. *J. Chromatogr. A* **2021**, *1649*, 462239. [[CrossRef](#)] [[PubMed](#)]
23. Yuan, C.; Jia, W.; Yu, Z.; Li, Y.; Zi, M.; Yuan, L.M.; Cui, Y. Are Highly stable covalent organic frameworks the key to universal chiral stationary phases for liquid and gas chromatographic separations? *J. Am. Chem. Soc.* **2022**, *144*, 891–900. [[CrossRef](#)] [[PubMed](#)]
24. Cui, Y.Y.; He, X.Q.; Yang, C.X.; Yan, X.P. Application of microporous organic networks in separation science. *TrAC-Trends Anal. Chem.* **2021**, *139*, 116268. [[CrossRef](#)]
25. Yang, Y.P.; Chen, J.K.; Guo, P.; Lu, Y.R.; Liu, C.F.; Wang, B.J.; Zhang, J.H.; Xie, S.M.; Yuan, L.M. A chiral porous organic polymer COP-1 used as stationary phase for HPLC enantioseparation under normal-phase and reversed-phase conditions. *Microchim. Acta* **2022**, *189*, 360. [[CrossRef](#)] [[PubMed](#)]
26. Tozawa, T.; Jones, J.T.A.; Swamy, S.I.; Jiang, S.; Adams, D.J.; Shakespeare, S.; Clowes, R.; Bradshaw, D.; Hasell, T.; Chong, S.Y.; et al. Porous organic cages. *Nat. Mater.* **2009**, *8*, 973–978. [[CrossRef](#)]
27. Mastalerz, M. Shape-persistent organic cage compounds by dynamic covalent bond formation. *Angew. Chem. Int. Ed.* **2010**, *49*, 5042–5053. [[CrossRef](#)]
28. Mastalerz, M. Porous shape-persistent organic cage compounds of different size, geometry, and function. *Acc. Chem. Res.* **2018**, *51*, 2411–2422. [[CrossRef](#)]
29. Hu, D.; Zhang, J.; Liu, M. Recent advances in the applications of porous organic cages. *Chem. Commun.* **2022**, *58*, 11333–11346. [[CrossRef](#)] [[PubMed](#)]
30. Jin, Y.; Voss, B.A.; Noble, R.D.; Zhang, W. A shape-persistent organic molecular cage with high selectivity for the adsorption of CO₂ over N₂. *Angew. Chem. Int. Ed.* **2010**, *49*, 6348–6351. [[CrossRef](#)]
31. Martínez-Ahumada, E.; He, D.; Berryman, V.; López-Olvera, A.; Hernandez, M.; Jancik, V.; Martis, V.; Vera, M.A.; Lima, E.; Parker, D.J.; et al. SO₂ capture using porous organic cages. *Angew. Chem. Int. Ed.* **2021**, *60*, 17556–17563. [[CrossRef](#)] [[PubMed](#)]
32. Yang, X.; Sun, J.K.; Kitta, M.; Pang, H.; Xu, Q. Encapsulating highly catalytically active metal nanoclusters inside porous organic cages. *Nat. Catal.* **2018**, *1*, 214–220. [[CrossRef](#)]
33. Gao, S.; Liu, Y.; Wang, L.; Wang, Z.; Liu, P.; Gao, J.; Jiang, Y. Incorporation of metals and enzymes with porous imine molecule cages for highly efficient semiheterogeneous chemoenzymatic catalysis. *ACS Catal.* **2021**, *11*, 5544–5553. [[CrossRef](#)]
34. Chen, G.J.; Xin, W.L.; Wang, J.S.; Cheng, J.Y.; Dong, Y.B. Visible-light triggered selective reduction of nitroarenes to azo compounds catalysed by Ag@organic molecular cages. *Chem. Commun.* **2019**, *55*, 3586–3589. [[CrossRef](#)] [[PubMed](#)]
35. Chen, L.; Reiss, P.S.; Chong, S.Y.; Holden, D.; Jelfs, K.E.; Hasell, T.; Little, M.A.; Kewley, A.; Briggs, M.E.; Stephenson, A.; et al. Separation of rare gases and chiral molecules by selective binding in porous organic cages. *Nat. Mater.* **2014**, *13*, 954–960. [[CrossRef](#)] [[PubMed](#)]
36. Xu, T.; Wu, B.; Hou, L.; Zhu, Y.; Sheng, F.; Zhao, Z.; Dong, Y.; Liu, J.; Ye, B.; Li, X.; et al. Highly ion-permselective porous organic cage membranes with hierarchical channels. *J. Am. Chem. Soc.* **2022**, *144*, 10220–10229. [[CrossRef](#)] [[PubMed](#)]
37. Su, K.; Wang, W.; Du, S.; Ji, C.; Yuan, D. Efficient ethylene purification by a robust ethane-trapping porous organic cage. *Nat. Commun.* **2021**, *12*, 3703. [[CrossRef](#)] [[PubMed](#)]

38. Dai, C.; Gu, B.; Tang, S.P.; Deng, P.H.; Liu, B. Fluorescent porous organic cage with good water solubility for ratiometric sensing of gold(III) ion in aqueous solution. *Anal. Chim. Acta* **2022**, *1192*, 339376. [[CrossRef](#)] [[PubMed](#)]
39. Lu, Z.; Lu, X.; Zhong, Y.; Hu, Y.; Li, G.; Zhang, R. Carbon dot-decorated porous organic cage as fluorescent sensor for rapid discrimination of nitrophenol isomers and chiral alcohols. *Anal. Chim. Acta* **2019**, *1050*, 146–153. [[CrossRef](#)] [[PubMed](#)]
40. Dai, C.; Qian, H.L.; Yan, X.P. Facile room temperature synthesis of ultra-small sized porous organic cages for fluorescent sensing of copper ion in aqueous solution. *J. Hazard. Mater.* **2021**, *416*, 125860. [[CrossRef](#)] [[PubMed](#)]
41. Dong, J.; Pan, Y.; Yang, K.; Yuan, Y.D.; Wee, V.; Xu, S.; Wang, Y.; Jiang, J.; Liu, B.; Zhao, D. Enhanced biological imaging via aggregation-induced emission active porous organic cages. *ACS Nano* **2022**, *16*, 2355–2368. [[CrossRef](#)] [[PubMed](#)]
42. Liu, H.; Duan, X.; Lv, Y.K.; Zhu, L.; Zhang, Z.; Yu, B.; Jin, Y.; Si, Y.; Wang, Z.; Li, B.; et al. Encapsulating metal nanoclusters inside porous organic cage towards enhanced radio-sensitivity and solubility. *Chem. Eng. J.* **2021**, *426*, 130872. [[CrossRef](#)]
43. Zhang, J.H.; Xie, S.M.; Chen, L.; Wang, B.J.; He, P.G.; Yuan, L.M. Homochiral porous organic cage with high selectivity for the separation of racemates in gas chromatography. *Anal. Chem.* **2015**, *87*, 7817–7824. [[CrossRef](#)] [[PubMed](#)]
44. Li, H.X.; Xie, T.P.; Yan, K.Q.; Xie, S.M.; Wang, B.J.; Zhang, J.H.; Yuan, L.M. A hydroxyl-functionalized homochiral porous organic cage for gas chromatographic separations. *Microchim. Acta* **2020**, *187*, 269. [[CrossRef](#)] [[PubMed](#)]
45. Xie, S.M.; Zhang, J.H.; Fu, N.; Wang, B.J.; Hu, C.; Yuan, L.M. Application of homochiral alkylated organic cages as chiral stationary phases for molecular separations by capillary gas chromatography. *Molecules* **2016**, *21*, 1466. [[CrossRef](#)] [[PubMed](#)]
46. Wang, Y.; Li, H.X.; Xie, S.M.; Wang, B.J.; Zhang, J.H.; Yuan, L.M. A [3 + 6] prismatic homochiral organic cage used as stationary phase for gas chromatography. *Microchem. J.* **2021**, *170*, 106650. [[CrossRef](#)]
47. Zhang, J.H.; Xie, S.M.; Zi, M.; Yuan, L.M. Recent advances of application of porous molecular cages for enantioselective recognition and separation. *J. Sep. Sci.* **2020**, *43*, 134–149. [[CrossRef](#)] [[PubMed](#)]
48. Wang, Y.; Chen, J.K.; Xiong, L.X.; Wang, B.J.; Xie, S.M.; Zhang, J.H.; Yuan, L.M. Preparation of novel chiral stationary phases based on the chiral porous organic cage by thiol-ene click chemistry for enantioseparation in HPLC. *Anal. Chem.* **2022**, *94*, 4961–4969. [[CrossRef](#)]
49. Kolb, H.C.; Finn, M.G.; Sharpless, K.B. Click chemistry: Diverse chemical function from a few good reactions. *Angew. Chem. Int. Ed.* **2001**, *40*, 2004–2021. [[CrossRef](#)]
50. Chu, C.; Liu, R. Application of click chemistry on preparation of separation materials for liquid chromatography. *Chem. Soc. Rev.* **2011**, *40*, 2177–2188. [[CrossRef](#)]
51. Petryk, M.; Szymkowiak, J.; Gierczyk, B.; Spólnik, G.; Janiak, A.; Kwit, M. Chiral, triformylphenol-derived salen-type [4+6] organic cages. *Org. Biomol. Chem.* **2016**, *14*, 7495–7499. [[CrossRef](#)] [[PubMed](#)]
52. Siles, B.A.; Halsall, H.B.; Dorsey, J.G. Retention and selectivity of flavanones on homopolypeptide-bonded stationary phases in both normal-and reversed-phase liquid chromatography. *J. Chromatogr. A* **1995**, *704*, 289–305. [[CrossRef](#)] [[PubMed](#)]
53. Yang, C.X.; Yan, X.P. Metal-organic framework MIL-101 (Cr) for high-performance liquid chromatographic separation of substituted aromatics. *Anal. Chem.* **2011**, *83*, 7144–7150. [[CrossRef](#)] [[PubMed](#)]
54. Anderson, A.A.; Goetzen, T.; Shackelford, S.A.; Tsank, S.A. Convenient one-step synthesis of 2-hydroxy-1,3,5-benzenetricarbaldehyde. *Synth. Commun.* **2000**, *30*, 3227–3232. [[CrossRef](#)]

Disclaimer/Publisher's Note: The statements, opinions and data contained in all publications are solely those of the individual author(s) and contributor(s) and not of MDPI and/or the editor(s). MDPI and/or the editor(s) disclaim responsibility for any injury to people or property resulting from any ideas, methods, instructions or products referred to in the content.